ELSEVIER

Journal of Pharmaceutical and Biomedical Analysis
13 (1995) 869–877

JOURNAL OF
PHARMACEUTICAL
AND BIOMEDICAL
ANALYSIS

Simulation of fractograms of fat emulsions in power-programmed sedimentation field-flow fractionation (SdFFF)

Shulamit Levin [a,*], Raphael Nudelman [a], Pierluigi Reschiglian [b], Luisa Pasti [c]

[a] *Pharmaceutical Chemistry Department, School of Pharmacy, P.O.B. 12065, The Hebrew University of Jerusalem, Jerusalem 91120, Israel*

[b] *Department of Chemistry "G. Ciamician", The University of Bologna, via Selmi 2, 40126 Bologna, Italy*

[c] *ECP EniChem Polimeri, Piazzale Privato G. Donegani 12, I-44100 Ferrara, Italy*

Received for review 22 July 1994; revised manuscript received 21 November 1994

Abstract

A quasi-empirical approach to the simulation of fractograms was examined to verify that the elution behavior of emulsions in power-based field programmed sedimentation field-flow fractionation (SdFFF) is consistent and predictable. The approach was applied to Intralipid, a commercial soybean emulsion and to an investigational medium chain triglyceride emulsion. The simulations predicted the fractograms that were obtained under various conditions of field strength, field decay and velocity of the suspending fluid, using distribution parameters obtained from one preliminary measurement of size distribution profile. Predicted fractograms were compared to experimental ones, under various fractionating powers. Good agreement was observed in most cases, in which interference of the secondary relaxation effects was not effective. The agreement confirmed the applicability of the approach to emulsions and that the simulations can be used instead of actual experiments for the optimization of their characterization by power-programmed SdFFF.

Keywords: Field decay; Fractogram; o/w emulsions; Power-programmed; Sedimentation field-flow fractionation; Simulation; Size distribution

1. Introduction

Colloids such as oil droplets in emulsions are developed to solubilize drugs, control their release, improve their durability in the living body and target them to the site of action whenever possible [1,2]. Long term stability, durability in the circulation system and sustained release of drugs are basic requirements from colloidal drug carriers. Some of the properties that qualify emulsions to carry drugs are the mean diameter of their oil droplets, as well as the polydispersity and the modality of their size distribution. For example, long term stability is effected by the polydispersity and modality of size distribution. Properties such as durability in complex media, kinetics of the release and targeting of the drugs also depend on the mean size distribution of the droplets [3]. Characterization of size distribution of emulsions and stability tests are done using spectroscopic and microscopic analyzers and various imaging counters [1,2,4].

Sedimentation field-flow fractionation (SdFFF) has also been shown to be a feasible analytical technique for the characterization of emulsions [5–9]. It is an analytical separation technique in which the selective elution along an ultra-thin channel is affected by a field perpendicular to the flow axis. The selective

* Corresponding author.

SSDI 0731-7085(95)01313-X

elution of colloids in the sedimentation mode of FFF is based on differences in their density and diameter, under the influence of the sedimentation field. The basic mechanism of the normal mode of retention in SdFFF has been described numerous times in the FFF literature; therefore, only a short explanation will be given here for clarification.

The clouds of droplets, which are formed under the influence of the sedimentation field, move downstream at a velocity proportional to their mean thickness. The more compressed they are to the wall, the slower they move. Droplets of different sizes form clouds of different thicknesses, and move downstream at different velocities; thus, separation takes place. The experimental data appear in the form of the detector response as a function of time, i.e. the fractogram. The exact relationship between the retention times and the respective retention parameters, λ, from which the diameters are calculated, has been described in many SdFFF publications [5]. The currently available SdFFF instruments manipulate the experimental data automatically. Diameters of the sample components are calculated from their retention data, and the relative mass for each diameter is calculated according to the procedure described by Yang et al. [5]. The result is a profile of size distribution.

SdFFF has been shown to be highly reproducible and accurate in giving the size distribution profile of oil droplets in polydisperse emulsions under either a constant field [5–7] or a decaying field [8,9]. It was shown that various conditions of the sedimentation field strength and rate of field decay, which were chosen arbitrarily, yielded identical size distribution of emulsions [8,9].

A quasi-empirical approach is applied here, which was first described for environmental samples, using power-based field decay by Reschiglian et al. [10]. The learning step utilizes experimental input, the average diameter and standard deviation of the oil droplets, obtained from a preliminary SdFFF run. The simulation then predicts the fractogram that would have been obtained under any given conditions of field strength, field decay and velocity of the mobile fluid. This numerical simulation can be used in principle as a learning tool and a powerful aid for the choice of the appropriate conditions of the analysis.

The object of this paper is to establish the applicability of this approach to emulsions. A good agreement between the simulated and experimental fractograms under various conditions of the analysis would confirm that their elution behaviour in SdFFF is consistent and predictable. Such consistency will allow the implementation of the simulated fractograms of emulsions as optimization tools for power-programmed SdFFF instead of running actual experiments.

2. Theory

2.1. Power-based field programming

The field programming used here for the two types of emulsions was power-based field decay [11,12]. In this programming of field strength, the initial field S_0 is held constant for t_1 (time-lag). Subsequently, the field strength is decreased over a chosen period of time until it is set at a prechosen constant value ($1g$ in this study). After t_1 has elapsed (where $t > t_1$) the field behaves according to the expression:

$$S(t) = S_0\left(\frac{t_1 - t_a}{t - t_a}\right)^p \tag{1}$$

where $S(t)$ is the field strength at time t, p is the variable of the power program and t_a is the decay constant ($t_a = -pt_1$). The resolving power is char-acterised by the fractionating power, F_d, the resolution between two closely eluting particles ($\delta t_R / 4\sigma_t$) divided by the differences in their relative diameter:

$$F_d = \frac{\delta t_R / 4\sigma_t}{\delta d / d} \tag{2}$$

where t_R is the retention time, σ_t is the standard deviation in retention time for particles of diameter d and $d + \delta d$ (where δd is the difference in diameter between the two neighboring particles). As reported, F_d is uniform over a wide range of diameters for a particular rate of field decay [12]. Eq. (44) in Ref. [12] describes the full expression of fractionating power F_d. In the presently operating SdFFF system where $n = 3$ and $p = 8$, it can be reduced to the following equation:

$$F_d = 0.171\,\frac{(Dt^0)^{1/2}}{w}\left(\frac{1}{\lambda_0}\right)^{1/6}\left(\frac{t_1 - t_a}{t^0}\right)^{4/3} \tag{3}$$

where D is the diffusion coefficient, which can be calculated from the Stokes–Einstein equation using the measured d, t^0 is the void time, and λ_0 is the retention parameter under the

initial field. The value of F_d depends on the initial field strength (S_0), t_1 and t_a, as well as the carrier velocity (through the void time t^0).

Once it is shown that the numerically simulated fractograms reflect the experimental ones, the simulation can be used in the future as an aid for the choice of the maximum fractionating power at a minimal analysis time.

2.2. Band broadening

The detector response as a function of time (fractogram) describes a large, widespread band of the fat emulsion. The eluting band of droplets assumes a finite width, which can be used to characterize their size distribution. The extent of dispersion of a sample zone, as a result of migration along the channel length L, under the influence of the perpendicular field, is termed the *plate height*, H, or *height equivalent to a theoretical plate*, HETP. For uniform channels $H = \sigma^2/L$ (where σ^2 is the variance of the profile).

The accurate measurement of peak dispersion is complex, but its elucidation is necessary in order to obtain an accurate size distribution profile. The two major contributions to the process of peak broadening due to non-equilibrium effects and sample polydispersity are given in the following equations [5]:

$$H = B\langle v\rangle + C \quad (4)$$

$$B = 3\pi\eta dw^2 24\lambda^3/kT \qquad C = 9L(\sigma_d/d_p)^2 \quad (5)$$

where $\langle v\rangle$ is the average linear velocity of the flowing streams and σ_d/d_p is the sample polydispersity. The term B describes the non-equilibrium contribution under a constant field and the term C describes the contribution due to the polydispersity in the size of the sample components. A typical apparent σ_d/d_p value was 0.45 for Intralipid and 0.22 for the medium chain triglyceride (MCT) emulsion (Table 1). The contribution of non-equilibrium effects that constitutes the first term in the equation is highly sensitive to the retention parameter λ, and is larger under a constant field. When the polydispersity is as high as the above σ_d/d_p, it becomes the major contributor to the band profile, while the dispersion due to non-equilibrium effects becomes negligible, especially in field decay. The shape of the profile of size distribution then remains invariant at various flow rates and no deconvolution of the two contributions (Eqs. (4) and (5)) is essential for accurate results, as was shown for both Intralipid and the MCT emulsion [8,9].

Table 1
Results from the fit of the profiles of size distribution of Intralipid and MCT emulsions to a Gaussian distribution

Emulsion	d_{mean} (μm)	σ_d	σ_d/d_{mean}
Intralipid I	0.387	0.165	0.43
Intralipid II	0.377	0.163	0.43
MCT	0.193	0.04	0.21

In addition to the invariability at different flow rates, the following experiment also indicated that polydispersity dominated the profile of size distribution [8,9]. Fractions were collected from the broad eluting FFF bands, and analyzed by photon correlation spectroscopy (PCS) [8,9]. When non-equilibrium effects contributed to the shape of the FFF band, the apparent FFF diameters of the droplets in the fractions prior to the peak maximum were underestimated by the SdFFF instrument, while those following the peak maximum were overestimated. The agreement between the FFF and PCS diameters on both sides of the peak maximum confirmed that the sample components were driven away from the maximum of the FFF band, owing to differences in their size rather than to non-equilibrium effects [8,9].

A good fit between the uncorrected experimental fractogram and the simulated one would also show that polydispersity dominates the band width.

2.3. Simulation of fractograms

The principle of the calculation of the fractogram was based on the assumption that its broad band describes an envelope of monodisperse micro-elements, each Gaussian in shape. The retention times and standard deviations were calculated for elution under power field decay, using the expressions presented by Williams and Giddings [12]. The peak shape of each micro-element was expressed as follows:

$$f_1(t, t', \sigma_t) = \frac{1}{(2\pi\sigma_t^2)^{1/2}} e^{-1/2(t-t'/\sigma_t)^2} \quad (6)$$

where t' is the mean retention time and σ_t is the standard deviation (time units), both functions of the particle diameter given the density value. The complete calculated fractogam is constructed using a weighting function that

combines the Gaussian monodisperse micro-elements with a Gaussian-shaped polydispersity function:

$$h_J(t) = \sum_i^K fi(t, t', \sigma_t) \times \frac{W_J}{(2\pi\sigma_{d_J})^{1/2}} e^{-1/2(d_J - d'_J/\sigma_{d_J})^2} \Delta J \quad (7)$$

where $h_J(t)$ is a dispersed single component peak shape, w_J is an amount coefficient, d'_J the average diameter, σ_{d_J} is the relative standard deviation and ΔJ is defined as follows:

$$\Delta J = \sigma_{d_J}/K \quad (8)$$

Fifty micro-elements ($K = 50$) were used for the construction of the band in this study. A good fit of the experimental band profile to the simulated one would indicate that the assumption of a Gaussian distribution of the oil droplets is valid.

3. Experimental

All the experimental conditions, material, instrumentation and procedure that were used to obtain the droplet size distribution were detailed previously for Intralipid [8], and for the MCT emulsion [9]; therefore, only experimental details relevant to the present approach will be given here.

3.1. Materials

The fractograms were taken from a previous study of two types of emulsions. One was a commercial soybean oil Intralipid (density = 0.92 g m^{-1} at 25 °C), which is marketed by Kabi Vitrum (Sweden) for intravenous nutrition; Intralipid I, expiration date 1991; Intralipid II, expiration date 1993 [9]. The second type of emulsion was made of MCTs ranging from 8 to 10 carbons that were obtained from the Societé des Oleagineux (Saint Blangy, France). The formulation was described in detail in a previous publication [8]. The density of the oil, reported by the manufacturer, was 0.940–0.950. A value of 0.945 was reported in the literature [13].

The mobile fluid in the SdFFF system was made up of 2.25% (w/v) glycerin in double distilled water with 0.0125% (w/v) sodium azide added as bactericide (refractive index 1.33, close to that of water). It was filtered through a 0.2 μm filter before use. The density of the solution was determined by pycnometer as 1.005 g ml^{-1}.

3.2. Instrumentation

A basic unit of particle and colloid fractionator, SedFFF model S101, equipped with a data station and control of RPM, capable of data acquisition and processing from FFFractionation Inc. (Salt-Lake City, UT), was used for the experimental fractograms. A 880-PU HPLC pump (Jasco, Japan) was used for MCT emulsion and a Varian 8500 (Pala Alto, CA) volumetric pump was used for Intralipid. A UV detector model UV-1 (Pharmacia, Bromma, Sweden), and a spectrophotometric detector model LC-85B from Perkin-Elmer (Norwalk, CT, USA) were operated at 254 nm for Intralipid and the MCT emulsion respectively. The channel dimensions were 2 cm in breadth, 0.0254 cm in thickness and 90 cm in length. The radius of the rotor was 15.1 cm. The void volume, measured using various small molecular weight substances, was 4.6 ml. The stop-flow was 20 min in the experiments with Intralipid and 40 min in the experiments with the MCT emulsion, apart from the operation with a constant field.

3.3. Computation

The numerical output of the SEDFFF software from the data station was transformed to Apple Macintosh format and treated mathematically (smoothing, normalization to the peak maximum and fitting to a Gaussian distribution) and graphically, using Igor™, a graphing and data analysis software for Macintosh (Mac Classic II) by WaveMetrics (Lake Oswego, OR).

The simulations provided complete fractograms that begin from the void time, as detailed previously [10]. The following parameters can be supplied to the program as the input: geometrical parameters of the channel and the rotor; programming conditions S_0 (initial field strength), t_1 (duration of constant field), t_a, and fractionating power, F_d (optional, was not used here); sample properties d_{mean} (mean diameter), $\Delta\rho$ (difference in density between the oil and the suspending fluid), and σ_d (the standard deviation). The routine for retention parameters was a FORTRAN 77 compiled software, whose output data was used to gener-

ate the simulated fractograms through a BASIC compiled subroutine [10].

The total simulated fractogram can be built up from N sample components, each of which consisted of K monodisperse micro-elements. Since the population of oil droplets was relatively uniform in terms of composition, the density was assumed to be constant, and $N = 1$ was used in the calculations. The resulted fractogram, which depicts the relative amount of the sample components in the micro-elements as a function of time, was converted from a PC format to Apple Macintosh format (by File Exchange) for graphical and data processing.

The assumption that the density of the oil droplets was constant over the entire range of diameters was based on the notion that the surface-active components of the oil droplet, the phospholipids, do not contribute significantly to its density. It is well known that liposomes (phospholipid vesicles) are neutral buoyancy colloids [14]. It is usually assumed by the pharmaceutical technologists that the density of oil droplets is homogeneous [13,15].

It should also be pointed out here that steric [16] and secondary relaxation effects [17] were not taken into account in the calculations of retention parameters.

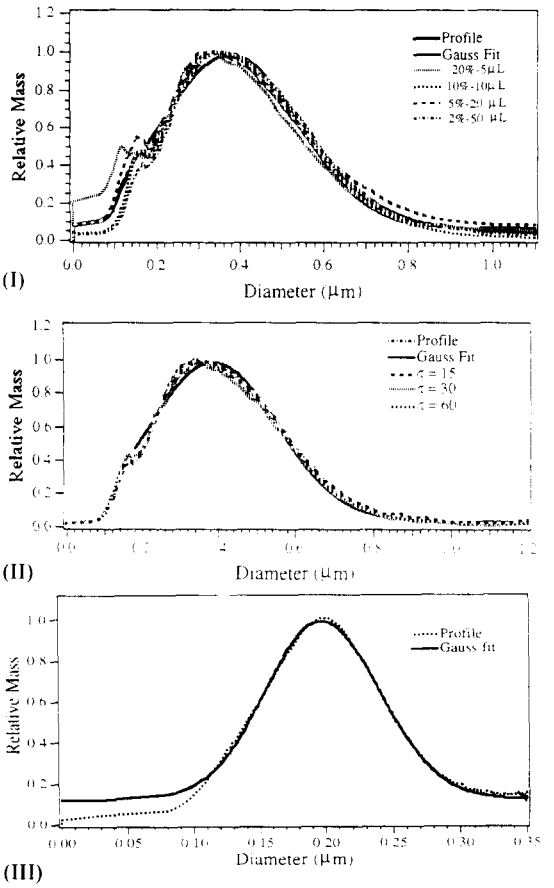

Fig. 1. The fit to a Gaussian function of the size distribution profiles of Intralipid and MCT emulsions. The average experimental size distribution profile of the two emulsions were taken from: (I) Intralipid I — four samples of Intralipid, containing a constant amount of oil droplets; (II) Intralipid II — runs using three different stop-flow times (τ) before elution, 15, 30 and 60 min; conditions — initial field was 108g (800 r.p.m.), final field 1g (75 r.p.m.), $t_f = 8$ min, $t_a = -64$ min and flow-rate 1.5 ml min^{-1}; (III) MCT — a constant field with stop-flow time 80 min. Field strength 169g (1000 r.p.m.) and flow-rate 2 ml min^{-1}.

4. Results and discussion

Three samples were studied. A commercial Intralipid from two different batches, and an investigational MCT emulsion, which was developed for drug carrying purposes [18,19]. The values of mean diameter, d_{mean}, and σ_d are needed as input values in the simulation of fractograms for any given programming conditions. Therefore, a size distribution profile that was obtained from a preliminary run was fitted to a Gaussian distribution, and the resulted statistical distribution parameters d_{mean} and σ_d were taken for the simulation of the fractograms. Table 1 presents the results of d_{mean} and σ_d of the size distribution profiles, and Figs. 1(I), 1(II), and 1(III) show the superposition of the experimental size distribution profiles with the corresponding fitted curves of the three emulsions that were studied here, Intralipid I, Intralipid II, and MCT respectively.

Visual inspection of the experimental and simulated fractograms reveals a reasonably good agreement between the curves, thus supporting the assumption of Gaussian distribution. The un-corrected raw experimental data were used in this study. In a more rigorous approach, the complex dependence of Mie scattering on the particle diameter and sample refractive index should be examined.

4.1. Intralipid I

The preliminary size distribution profile of Intralipid I that was used for the extraction of the distribution parameters was an average profile, obtained by injecting a constant sample load at various injection volumes, as reported in Ref. [9]. The feasibility of the simulation in the characterization of Intralipid I was tested by simulating fractograms of three runs using

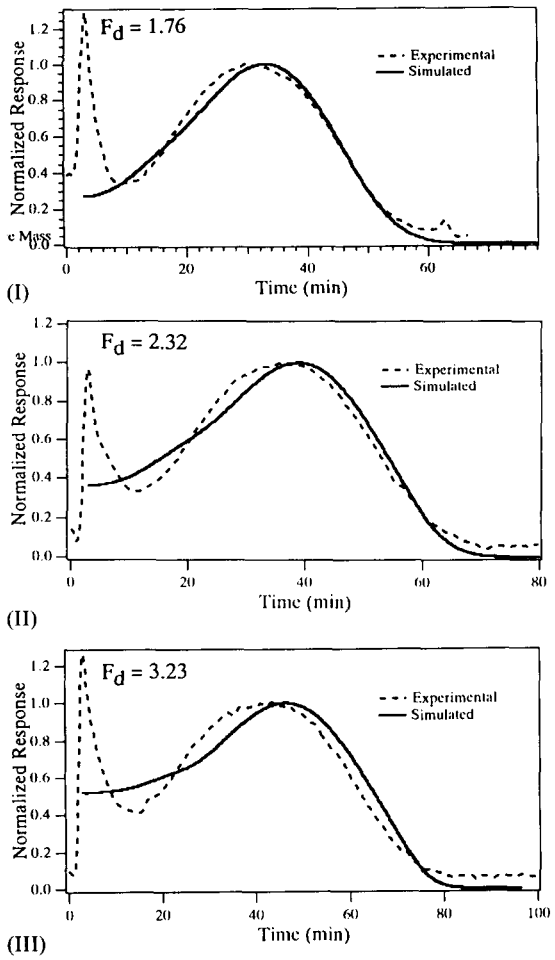

Fig. 2. Simulated vs. experimental fractograms of Intralipid I, using three different methods of field programming. (I) Program A ($t_1 = 8$ min and $t_a = -64$); (II) Program B ($t_1 = 10$ min and $t_a = -80$); (III) Program C ($t_1 = 13$ min and $t_a = -104$). Initial field strength was 108g, final field 1g and flow-rate 1.5 ml min^{-1}.

different values of initial time-lag period of the field decay (t_1), i.e. three different fractionating powers F_d.

The following programs were used in the experiment. Program A, $t_1 = 8$ min ($t_a = -64$ min); Program B, $t_1 = 10$ min ($t_a = -80$ min); Program C, $t_1 = 13$ min ($t_a = -104$ min). The rest of the experimental parameters, such as the initial (108g) and final (1g) field strengths, stop-flow time (20 min), and the rate of data acquisition (10 points min^{-1}), were identical in all three cases. Fig. 2 shows the calculated and the experimental fractograms using the three Programs A, B and C. The values of F_d corresponding to the different t_1 values are specified on the graphs.

4.2. Intralipid II

An average size distribution profile from repetitive measurements at various relaxation times (also described previously [9]) was used to obtain the input values for the simulations of Intralipid II. The feasibility of the simulation in characterizing Intralipid II was tested using Program A at three flow rates: 1, 1.5 and 2 ml min^{-1}. The calculated and experimental fractograms are shown in Figs. 3(I–III), respectively, in which the three values of F_d corresponding to the three flow-rates are also specified.

4.3. MCT emulsion

The distribution parameters of the simulations of the fractograms of MCT emulsion were obtained under a constant field, a run that has been described previously [8]. The MCT emulsion was clearly narrower and more regularly dispersed than the two Intralipid emulsions. The diameters of the oil droplets were approximately 50% smaller and, therefore, comparable analysis times and F_d values were obtained using a higher initial field strength (380g).

The agreement between the experimental and simulated fractograms of the MCT emulsion was tested using three field programs at 1.5 and 2 ml min^{-1}: Program A (see Intralipid I); Program B (see Intralipid I); Program D, $t_1 = 12$ min ($t_a = -96$). The rest of the experimental parameters, such as the initial (380g) and final (1g) field strengths, stop-flow time (40 min), and rate of data acquisition (10 points min^{-1}), were identical in the three programs. The superimposed calculated and experimental fractograms are shown in Figs. 4(I–III) and 5(I–III) for 1.5 and 2 ml min^{-1} respectively. The values of the fractionating powers F_d corresponding to the various conditions are specified in the Figures.

Visual inspection of Figs. 2–5 reveals that a reasonably good agreement between the experimental and calculated fractogtrams was obtained in most cases, confirming that the apparent profiles of size distribution that were used for the calculations were accurate. The experimental fractograms were slightly skewed, since no baseline corrections were made; therefore, there is a slight mismatch at the trailing edges of the curves.

The raw fractograms of the MCT emulsion in Figs. 4(I–III) and 5(I–III) were slightly

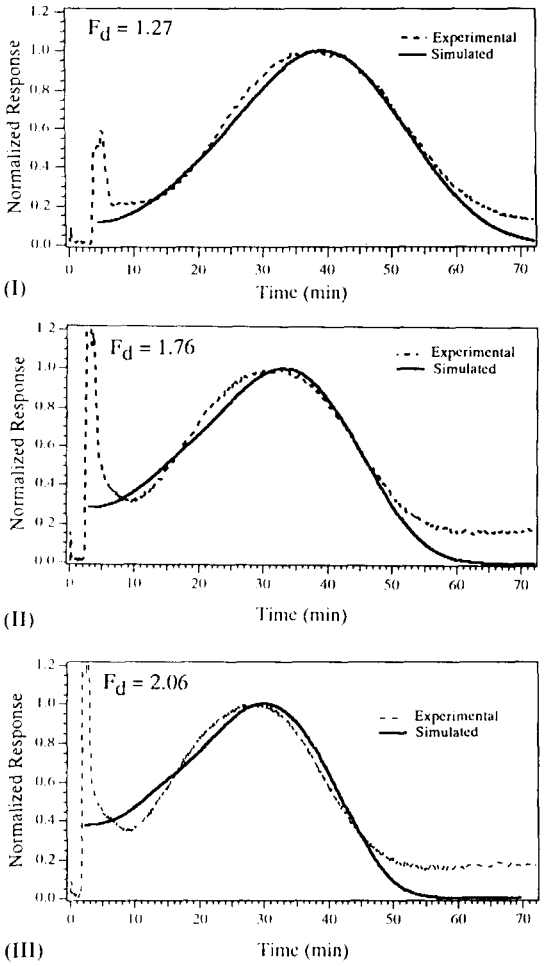

Fig. 3. Simulated vs. experimental fractograms of Intralipid II, obtained at three flow-rates. (I) 1 ml min^{-1}; (II) 1.5 ml min^{-1}; (III) 2 ml min^{-1}. Program A (see Fig. 2) was used; initial field 108*g*, final field 1*g*, stop-flow time = 20 min.

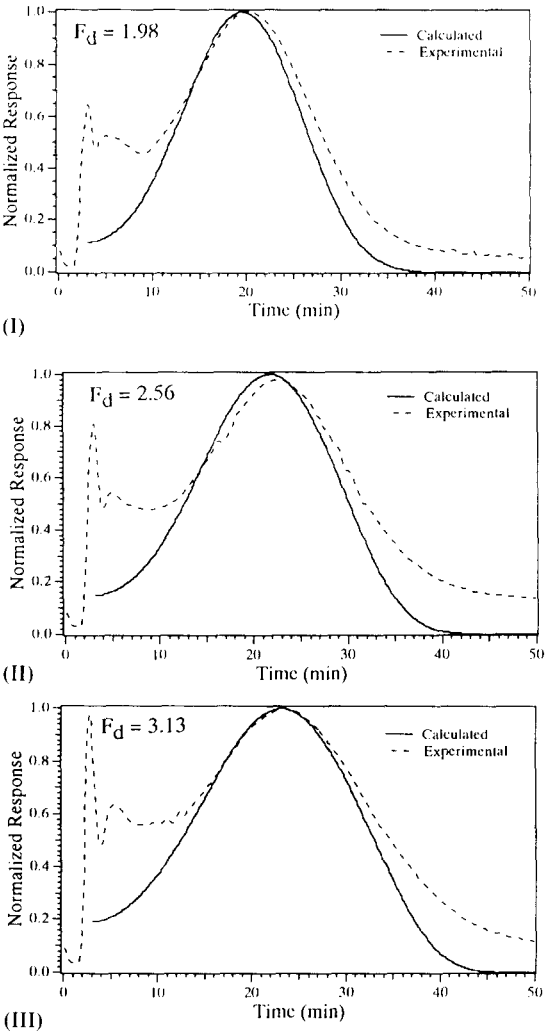

Fig. 4. Simulated vs. experimental fractograms of MCT emulsion, using three different programs. (I) Program A (see Fig. 2); (II) Program B (see Fig. 2); (III) Program D ($t_1 = 12$ min and $t_a = -96$). Initial field strength was 380*g* (RPM = 1500), final field 1*g*, flow-rate 1.5 ml min^{-1}.

broader than the calculated ones. The slight mismatch in peak width could be due to the fact that the experimental fractograms were obtained under field-decay, whereas the input value of σ of the profile of size distribution, used for the calculations, was obtained under a constant sedimentation field. Fine tuning of σ should improve the agreement between the curves.

In spite of the fact that raw experimental fractograms were used (not even baseline corrections), good agreement was obtained between the position of the simulated and the experimental peaks and reasonable agreement was obtained between their widths. This agreement establishes the consistency of the behavior of these rather complex and delicate samples in SdFFF under field-decay, showing that the approach is valid for development of a systematic optimization strategy in the future. The simulated fractograms can be used for the evaluation of the appropriate conditions of the analysis of emulsions with-out the need to actually run the experiments repeatedly.

4.4. Band broadening

The calculation of fractograms using the quasi-empirical approach described here took into account both non-equilibrium effects and polydispersity. The apparent σ_d of the raw size distribution profile was taken for the simulations with no deconvolution of the non-equilibrium effect. The agreement between the

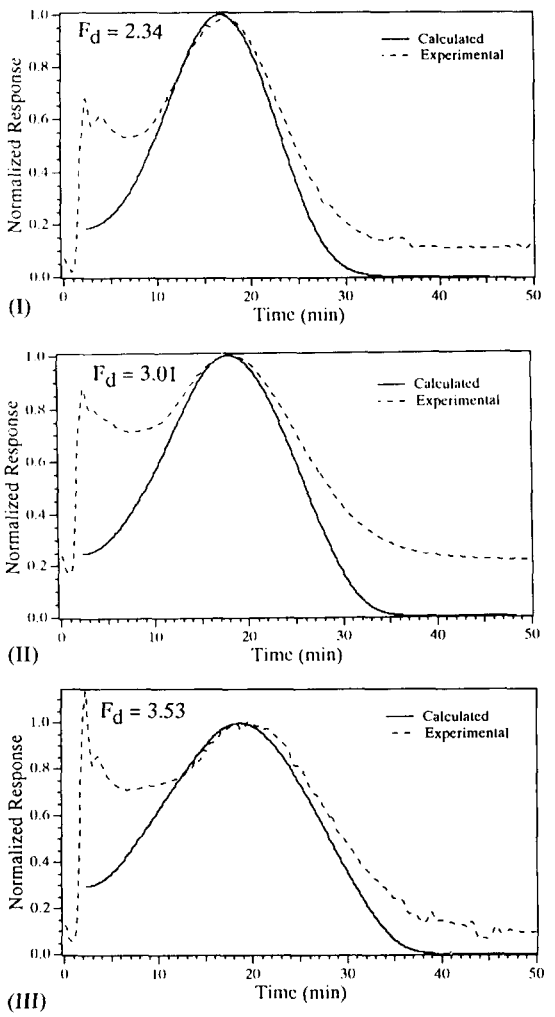

Fig. 5. Simulated vs. experimental fractograms of the MCT emulsion, using the same conditions as in Fig. 4, except for the flow-rate, which was 2 ml min^{-1}.

experimental and simulated fractograms of the fat emulsions therefore verifies that the band broadening was dominated by the polydispersity of the oil droplets. The simulation uses the apparent σ_d, and then adds the non-equilibrium effects. If the non-equilibrium effects were dominant, the simulated chromatogram would have been considerably broader than the experimental one. In cases where the fractogram is significantly effected by non-equilibrium effects, an iterative procedure can be used by feeding decreasing values of σ_d into the simulation program until the calculated and experimental bands coincide. At the end of such an iterative procedure the resulted specific value of σ_d would lead to a good agreement between the calculated and the experimental fractograms, and would reflect the actual polydispersity of the sample. This final σ_d can be used for further power-programmed simulations.

5. Conclusions

It was shown that the quasi-empirical approach presented here enabled the prediction of experimental fractogams using a pre-determined distribution profile. The mere fact that the simulated fractograms reflected the experimental ones promises that in a future thorough and comprehensive optimization procedure they can be used as an aid for the choice of the appropriate conditions of the analysis. The optimization of these conditions saves the need to actually run the sample under the various conditions.

Acknowledgments

This work was supported by the following funds of the Hebrew University of Jerusalem —"Leonie Emanual Fund", "Mary Gordon Fund" and "Ernst Chain Fund" — and by the Italian NCR, the program for scientists' exchange. We are grateful to Professor F. Dondi from the Chemistry Department at the University of Ferrara for his collaboration and support of the subject. We also thank Professor S. Benita, from the Pharmacy Department at the School of Pharmacy, The Hebrew University, for the emulsions and consultation.

References

[1] M.R. Rieger, in L. Lachman, H.A. Lieberman and J.L. Konig (Eds.), Theory and Practice of Industrial Pharmacy, Lea and Febiger, Philadelphia, PA, 1986, pp. 502–533.
[2] L.H. Block, in H.A. Liebermann, M.M. Rieger and G.S. Banker (Eds.), Pharmaceutical Dosage Forms, Marcel Dekker, New York, 1989, pp. 335–378.
[3] M.Y. Levy and S. Benita, Int. J. Pharm., 54 (1989) 103–112.
[4] C. Washington, Int. J. Pharm., 66 (1990) 1–21.
[5] F.-S. Yang, K.D. Caldwell, M.N. Myers and J.C. Giddings, J. Colloid Interface Sci., 93 (1983) 115–125.
[6] K.D. Caldwell and H. Li, J. Colloid Interface Sci., 132 (1989) 246–268.
[7] J. Li, K.D. Caldwell and B.D. Anderson, Pharm. Res., 10 (1993) 535–541.
[8] S. Levin, E. Klausner and S. Muchtar, J. Pharm. Biomed. Anal., 12 (1994) 1115–1121.
[9] S. Levin, L. Stern, A. Ze'evi and M.Y. Levy, Anal. Chem., 66 (1994) 368–377.

[10] P. Reschiglian, L. Pasti and F. Dondi, J. Chromatogr. Sci., 30 (1992) 217–227.
[11] P.S. Williams and J.C. Giddings, J. Chromatogr., 550 (1991) 787–797.
[12] P.S. Williams and J.C. Giddings, Anal. Chem., 59 (1987) 2038–2044.
[13] O. Lutz, Z. Meraihi, J.-L. Mura, A. Frey, G.H. Reiss and A.C. Bach, Am. J. Clin. Nutr., 50 (1989) 1370–1381.
[14] K.D. Caldwell, G. Karaiskakis and J.C. Giddings, Colloids Interfaces, 3 (1981) 233–238.
[15] D.H. Everett, Basic Principles of Colloid Science, Royal Society of Chemistry, London, 1988.
[16] M.N. Myers and J.C. Giddings, Anal. Chem., 54 (1982) 2284–2289.
[17] M.E. Hansen, J.C. Giddings, M.R. Schure and R. Beckett, Anal. Chem., 60 (1988) 1434–1442.
[18] J. Kleinstern, E. Markowitz and S. Benita, STP Pharm. Sci., 3 (1993) 163–169.
[19] M.Y. Levy, I. Polacheck, Y. Barenholz and S. Benita, J. Med. Vet. Mycol., 31 (1993) 207–218.